JTTEE5 19:303–310
DOI: 10.1007/s11666-009-9377-3
1059-9630/$19.00 © ASM International

Atmospheric Plasma Spraying of High Melting Temperature Complex Perovskites for TBC Application

M.O. Jarligo, D.E. Mack, G. Mauer, R. Vaßen, and D. Stöver

(Submitted April 30, 2009; in revised form July 14, 2009)

High melting materials have always been very attractive candidates for materials development in thermal barrier coating (TBC) applications. Among these materials, complex perovskites with $Ba(Mg_{1/3}Ta_{2/3})O_3$ and $La(Al_{1/4}Mg_{1/2}T_{1/4})O_3$ compositions have been developed and deposited in TBC systems by atmospheric plasma spraying. Spray parameters were optimized and in-flight particle temperatures were recorded using Accuraspray-g3 and DPV 2000. Plasma sprayed coatings were found to undergo non-stoichiometric decomposition of components which could have contributed to early failure of the coatings. Particle temperature diagnostics suggest that gun power of ~15 kW or lower where majority of the particles have already solidified upon impact to the substrate could probably prevent the decomposition of phases. Additionally, it has been found that the morphology of the powder feedstock plays a critical role during atmospheric plasma spraying of complex perovskites.

Keywords atmospheric plasma sprayed (APS) coatings, gas turbine coatings, particle diagnostics, perovskite ceramics

1. Introduction

One of the most essential requirements for advanced thermal barrier coating (TBC) materials of gas-turbine engines is phase stability at extremely high operation temperature (~1300 °C), in order to improve the engine efficiency and performance (Ref 1). The most promising candidates for materials development, therefore, are those with high melting temperatures in addition to phase stability and low thermal conductivity in general. Among these materials, $AB'_{1/3}B''_{2/3}O_3$ complex perovskite in particular with $Ba(Mg_{1/3}Ta_{2/3})O_3$ (BMT) composition has melting temperature of ~3000 °C and is considered among the most refractory oxides ever known to science (Ref 2, 3). This complex perovskite has a *B*-site cation dependent dual crystal structure which the material may adopt to maintain chemical stability, making it unique from other perovskites (Ref 3, 4). The B' and B'' cations can exhibit 1:2 ordering along the [111] axis forming a hexagonal $P\bar{3}m1$ space group symmetry typically found in well sintered ceramics. In some cases, the non-stoichiometric 1:1 ordering is preferred leading to a cubic $Fm\bar{3}m$ symmetry as found in single crystal BMT. Recently, the $La(Al_{1/4}Mg_{1/2}T_{1/4})O_3$ (LAMT) complex perovskite system has also gained research attention due to similar properties with BMT. Their bulk properties include low values of thermal conductivity (~2 W/m·K) and high coefficient of thermal expansion (~11 × 10^{-6}/K), which are promising for TBC applications (Ref 5).

For applicability in TBC systems, the deposition of these perovskite materials is often challenged by the formation of secondary phases during atmospheric plasma spraying (Ref 6-8). The secondary phases formed on atmospheric plasma spraying BMT and LAMT are however very stable and do not contribute to any significant structural changes of the complex perovskites as observed in consistent linear expansion profiles up to 1200 °C which are previously reported in Ref 5. Somehow, their presence caused an integral effect on the low thermal cycling lifetime of the coatings. Although the major cause of coating failure was reported to be oxidation driven due to further growth of a thermally grown oxide layer, it should be noted that the formation of these secondary phases is also oxidation driven. To avoid inhomogeneous coating properties, succeeding investigations are focused on preventing the formation of secondary phases during plasma spraying. To carry out the investigation, in-flight particle diagnostics is therefore a necessary tool to better understand the particle state during spraying.

The Accuraspray-g3 and DPV-2000 systems both from Tecnar Automation Ltd., Canada, are among the popular

This article is an invited paper selected from presentations at the 2009 International Thermal Spray Conference and has been expanded from the original presentation. It is simultaneously published in *Expanding Thermal Spray Performance to New Markets and Applications: Proceedings of the 2009 International Thermal Spray Conference*, Las Vegas, Nevada, USA, May 4-7, 2009, Basil R. Marple, Margaret M. Hyland, Yuk-Chiu Lau, Chang-Jiu Li, Rogerio S. Lima, and Ghislain Montavon, Ed., ASM International, Materials Park, OH, 2009.

M.O. Jarligo, D.E. Mack, G. Mauer, R. Vaßen, and **D. Stöver**, Institut für Energieforschung (IEF-1), Forschungszentrum Jülich GmbH, Jülich, Germany. Contact e-mail: m.o.jarligo@fz-juelich.de.

monitoring tools available for in-flight particle diagnostics. The Accuraspray-g3 system provides an average data representing the characteristics of an ensemble of particles in a measurement volume (~3 mm Ø by 25 mm). Particle velocities are obtained from the cross-correlation of signals which are recorded at two closely spaced locations. The system is also equipped with a CCD (charge-coupled device) camera that analyzes the plume appearance along a spray path perpendicular to the particle jet. The DPV-2000 system, on the other hand, enables the measurement of particle velocities obtained by measuring the time between two signals which are triggered by a radiating particle passing a two-slit mask of an optoelectronic sensor head attachment. Unlike the Accuraspray-g3, the measurement volume for DPV-2000 system is relatively small (<1 mm^3) and the data can be collected for individual particles and subsequently analyzed. The particle temperature is generated through two-color pyrometry for both monitoring systems. Details of the monitoring systems and their capabilities are described in Ref 9 and 10. In this paper, results on the investigation of the secondary phase formation on plasma spraying complex perovskite powders in sintered and crushed and spray dried forms are detailed in relation to the cycling lifetime of the TBCs, as well as the particle state in terms of velocity and temperature during flight in the plasma plume. Finally, process maps are also presented to identify the appropriate spray conditions which could avoid as much as possible the formation of secondary phases accompanying the usual plasma spraying process of perovskites.

2. Experimental Procedure

2.1 Powder Production

Single phase complex perovskites $Ba(Mg_{1/3}Ta_{2/3})O_3$ and $La(Al_{1/4}Mg_{1/2}T_{1/4})O_3$ were produced by a mechanically activated solid state route from powder mixtures of $BaCO_3$ (99.8%, Alfa Aesar, Germany), La_2O_3 (99.9%, Aldrich, Germany), Al_2O_3 (>95%, Fluka, Germany), MgO (>99%, Aldrich, Germany) and Ta_2O_5 (98.95%, Treibacher Powdermet, Austria) in ethanol. Milled suspensions were then oven-dried, calcined at 1250 °C and finally sintered at 1600 °C. The powders obtained were mechanically pulverized and classified as sintered and crushed. It is critical that the dried powders be well dispersed by proper sieving with at least 300 μm sieve prior to subsequent heat treatments, otherwise the resulting morphology of the sintered and crushed will not provide good feedstock flowability during plasma spraying as previously observed with LAMT. Spray dried powders were then produced by further milling the sintered and crushed with ethanol and 1.8 wt.% dispersing agent. Sieving subsequently followed to obtain only those passing 125 μm from each powder classification for use in coating preparation. Particle size distribution was then determined using a laser particle size analyzer (Analysette 22, Fritsch, Germany).

2.2 Coating Preparation

Deposition of the BMT coatings was carried out in an atmospheric plasma spray facility with a Triplex I gun (Sulzer Metco, Switzerland) operated with flowing argon and helium at 20 and 13 standard liter per minute (slpm), respectively, and a spray distance of 90 mm. For LAMT, Triplex II (Sulzer Metco, Switzerland) operated with flowing Ar and He at 45 and 6 slpm, respectively, with a spray distance of 150 mm was used since during optimization of spray parameters, deposition with Triplex I failed as reported in Ref 4. These optimized spray conditions had good deposition efficiency and were adopted as optimum standards for spraying with the respective spray torches and materials. The powders were deposited on standard steel plates which were previously sand-blasted. Free-standing coatings were then removed by soaking the coated steels with HCl. To determine the stability of the phases in the coatings after thermal spraying, the free-standing coatings were annealed at 1500 °C for 3 h at a heating rate of 5 °C per minute. This was conducted since rapid cooling during spraying leads to formation of metastable phases in the coating (Ref 11). Mercury porosimetry (Pascal 140, CE Instruments, Italy), x-ray diffraction (D4 Endeavor, Burke, Siemens, Germany) and scanning electron microscopy (SEM) (Ultra55, Zeiss, Germany) were then conducted. Thermal cycling samples were also prepared by depositing the powders on disk-shaped nickel-base superalloy IN738 substrates with NiCoCrAlY (Ni-192-8, Sulzer Metco, Switzerland) bondcoat. Double-layer systems consisting of a 7.8 wt.% yttria stabilized zirconia (YSZ) (APS Y239 M, Sulzer Metco, Switzerland) coating directly deposited on the bondcoat and a complex perovskite topcoat were also produced. A gas burner rig facility (IEF-1, Forschungszentrum Jülich GmbH, Germany) was used to determine the thermal cycling lifetime which is the number of thermal cycles at which visible spallation of about 5 × 5 mm^2 appears on the central region of the surface of the sample on repeated 5-min heating and 2-min cooling.

2.3 In-Flight Particle Diagnostics

The aim of this procedure is to determine the set of spray parameters and equipment which could generate the highest particle velocity and optimum particle temperature within allowable operational capacity of the spray systems in IEF-1, Forschungszentrum Jülich GmbH. In-flight measurements of particle temperatures for coatings deposited with the standard parameters were first conducted with Accuraspray-g3 to establish a baseline standard from which other spray parameters for particle diagnostics could be varied. Subsequent measurements were then carried out through atmospheric plasma spraying with three-cathode Triplex guns on a Multi-Coat controller (Sulzer Metco, Switzerland) and mounted on a six-axis robot (IRB2400, ABB, Sweden). Triplex II (9 mm nozzle) and Triplex-Pro guns with 6.5 and 9 mm nozzles (Sulzer Metco, Switzerland) were employed, while the DPV-2000 system was used as the particle monitoring

system to better generate individual particle data rather than ensemble data. The plasma gun employed is positioned in front of the optoelectronic sensor of the DPV-2000 system so that the measurement scope is within the spraying distance of the work piece. Before each measurement, the particle flow is scanned along the horizontal and vertical directions to determine the precise point (±0.1 mm accuracy) where particle flow rate is maximum. Data sets of approximately 2000 particles were recorded for about 30 s. The actual values were monitored and recorded continuously during the process. Further information of the monitoring techniques and data acquisition are detailed in Ref 9. The results are then summarized in process maps.

3. Results and Discussion

3.1 Powder Morphology

The morphology of the powder feedstock plays an important role in achieving high deposition efficiency of the powders during plasma spraying. Micrographs in Fig. 1 show the particle morphology of the powders, revealing irregular morphology common to sintered and crushed powders, and hollow spheres for the spray-dried particles. Figures 2 and 3 show that the particle size distributions of the spray-dried powders are narrower than that of the sintered and crushed powders, indicating a more homogeneous size distribution. The narrow range is advantageous in achieving good flowability of the powder feedstock and control of the trajectory distribution, since particle collisions with the powder injector wall and among themselves during spraying drastically increase if their size is below 20 μm. This result to more divergent trajectories and feeding problems such as clogging (Ref 12-14).

The spray dried powders in Fig. 2 and 3 appear to have higher powder volume with larger size compared to the sintered and crushed powders. It should be noted, however, that every agglomerated sphere will be totally dispersed in the plasma plume during injection, hence the actual in-flight particle size is in fact smaller. The probability of material decomposition is higher compared to the larger particles from sintered and crushed powders as reported in Ref 14.

3.2 Coating Properties

Spray dried BMT and LAMT powders deposited using the optimized standard spray parameters, produced coatings with porosity of about ~17 and 13%, respectively. SEM micrographs of the coatings in Fig. 4 reveal more horizontal intersplat cracks in the BMT coating as compared to the higher concentration of vertical crack networks in the LAMT coatings. Also visible are thin white shades of the secondary phases (indicated by arrows) determined by EDX (energy-dispersed x-ray analysis) to

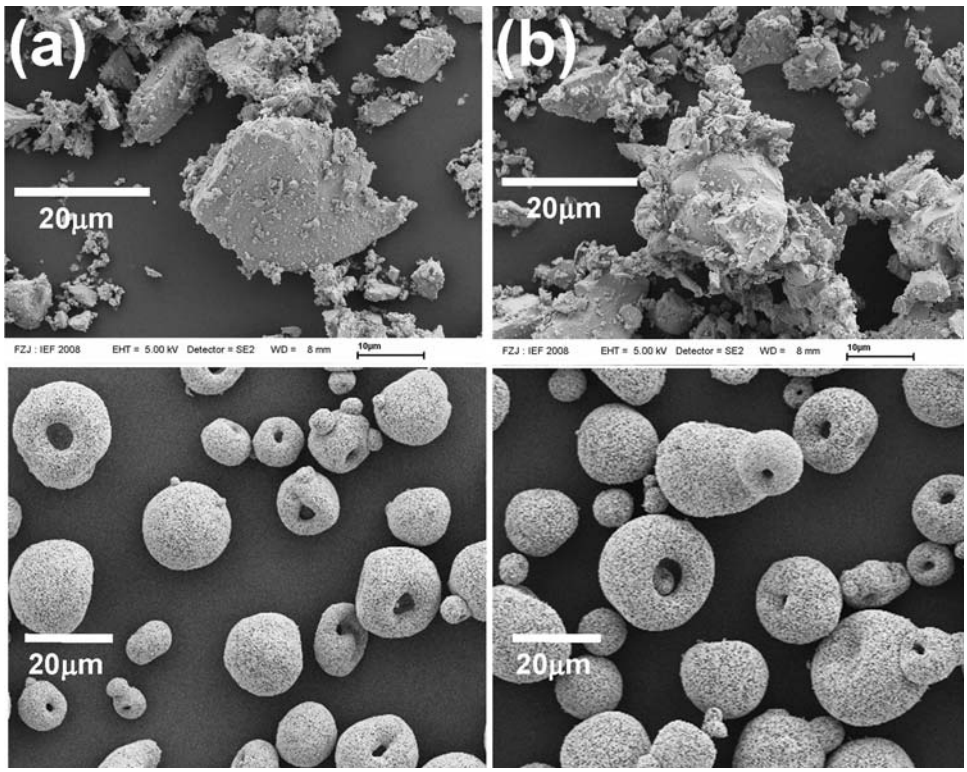

Fig. 1 SEM micrographs of the sintered and crushed powders of (a) BMT and (b) LAMT; below are the corresponding spray-dried powders

be composed of Ba, Ta and O for the BMT coating and La, Ta, O for the LAMT coating. The secondary phases still appear even after annealing at 1500 °C. These findings are confirmed by the x-ray diffraction profiles in Fig. 5 and 6. The starting powder (Fig. 5a) has a hexagonal perovskite structure which rearranges to cubic form in the as-sprayed coating (Fig. 5b) as an effect of rapid cooling and simultaneous material decomposition during plasma spraying. On annealing, the material reverts to hexagonal BMT (Fig. 5c), although secondary phase still remained in the coating. The BMT secondary phase $Ba_3Ta_5O_{15}$ (BTO) also has a hexagonal structure and is known to be very

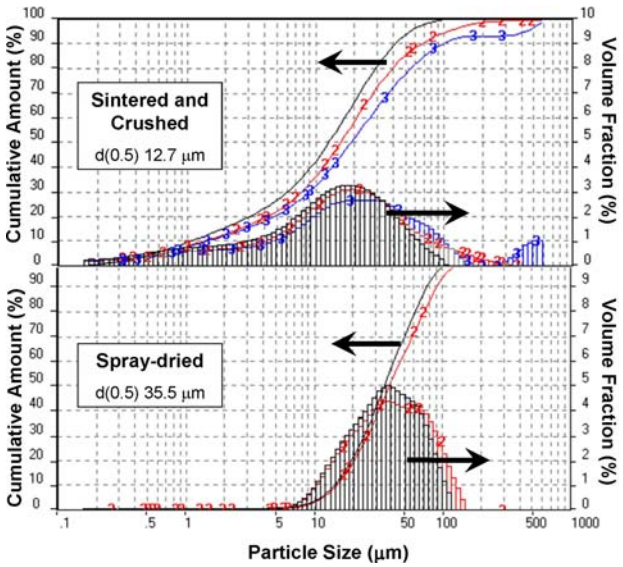

Fig. 2 Particle size distribution of BMT

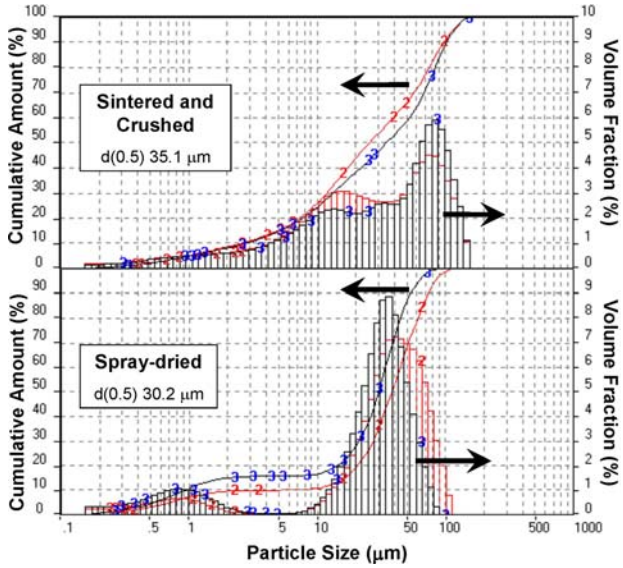

Fig. 3 Particle size distribution of LAMT

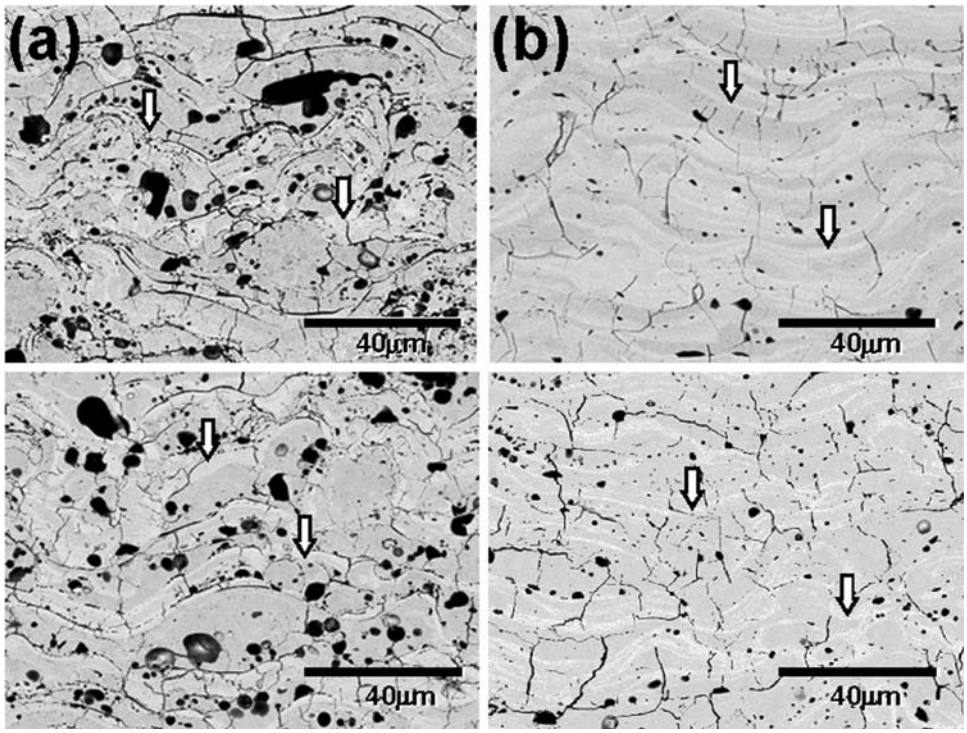

Fig. 4 SEM micrographs of plasma sprayed (a) BMT and (b) LAMT powders; below are corresponding coatings annealed at 1500 °C for 3 h

stable even when sintered at temperatures higher than 1600 °C for long periods of time (Ref 15). The formation of BTO is due to the loss of oxide components of Ba and Mg during spraying as confirmed by the chemical analysis of the plasma sprayed coatings. Hence, BMT composition was reformulated with excess Ba and Mg to compensate for the amount that would be lost during spraying. X-ray diffraction profiles for LAMT reveal similar cubic-hexagonal transformation of the as-sprayed (Fig. 5d) and annealed (Fig. 5e) coatings. Although the as-sprayed

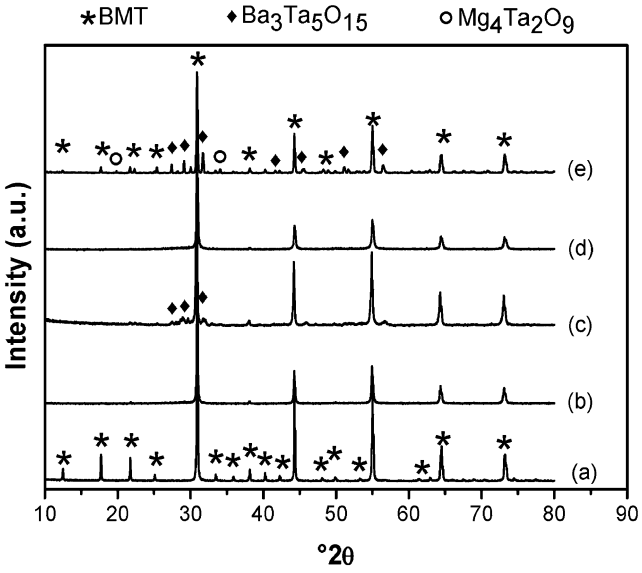

Fig. 5 X-ray diffraction profiles of BMT produced with stoichiometric starting composition; (a) powder form, (b) as-sprayed coating and (c) annealed coating at 1500 °C, while the non-stoichiometric composition with excess Ba and Mg are (d) as-sprayed coating and (e) annealed coating at 1500 °C

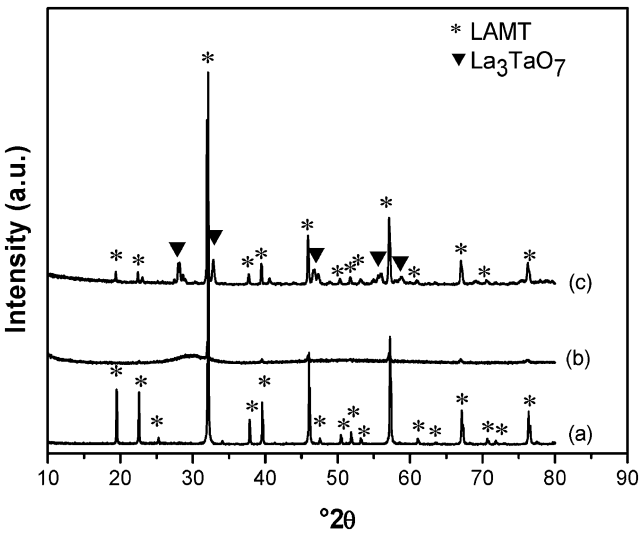

Fig. 6 X-ray diffraction profiles of LAMT produced with stoichiometric composition; (a) powder form, (b) as-sprayed coating and (c) annealed coating at 1500 °C

LAMT coating appears to be single phase, the annealed coating shows that additional secondary phases are formed.

3.3 Coating Lifetime

Thermal cycling test results in Fig. 7 show that $Ba(Mg_{1/3}Ta_{2/3})O_3$ coatings prepared from sintered and crushed powders have longer lifetime compared to that from the spray-dried powders. This is probably due to the deposition efficiency of the powders, in that fine constituents of the agglomerated spray-dried may have experienced excessive decomposition and have already cooled down before hitting the substrate or may have not enough inertia to hit the substrate and flatten as compared to the sintered and crushed powders (Ref 16). Details for coating lifetime of complex perovskites are discussed in Ref 5.

3.4 Particle Temperature

Figure 8 summarizes the in-flight particle characteristics. Sintered and crushed powders were used for the

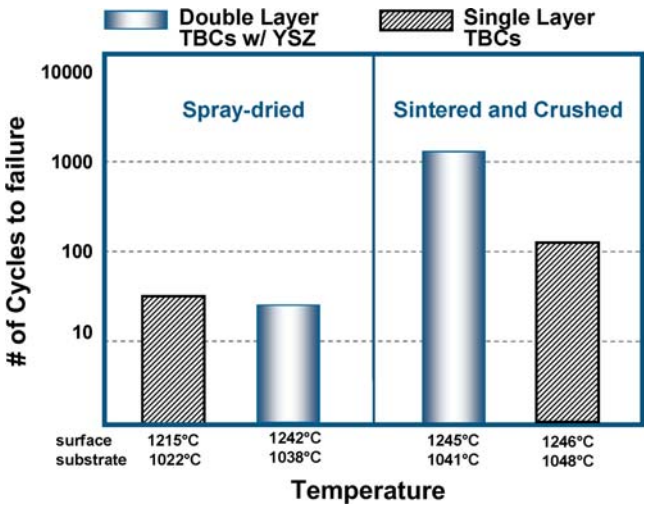

Fig. 7 Thermal cycling lifetime of BMT complex perovskite coatings prepared from different particle morphologies

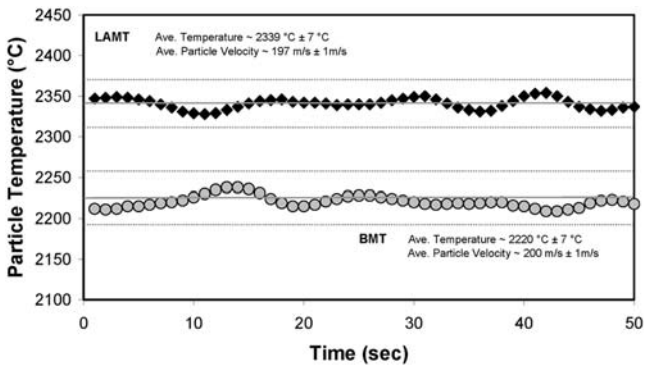

Fig. 8 In-flight particle characteristics of BMT and LAMT generated from measurements with Accuraspray-g3

diagnostics, deriving from the benefit of achieving higher cycling lifetime with this powder form. It should be noted that the diagnostics data were obtained with Accuraspray-g3 which averages the characteristics of an ensemble of particles at a given observation volume. The obtained particle temperatures and velocity from the standard spray parameters used will be made as basis for further process optimization with the aim of eliminating the secondary phases in the coatings.

3.5 Process Maps

The major aim of generating process maps is to determine spray parameters which can generate the fastest particles possible to avoid decomposition at the melting temperature. Additionally, such spray parameters should as well as attain enough particle temperature to obtain a molten state at least on the surface of the particle to achieve an efficient coating deposition based from the previously optimized standards. Consequently, high particle velocity was found to effectively minimize the effect of unnecessary reactions during spraying (Ref 17).

The spray parameters used for BMT are summarized in Table 1 and the results generated with the DPV-2000 system are summarized in the process map shown in Fig. 9. Parameter set #16 is the previously optimized parameter set as standard when spraying with the Triplex II gun which has a standard 9 mm nozzle. The first approach in selecting a small nozzle (6.5 mm diameter) for the gun was to achieve higher particle velocity than with Triplex II. However, this was not successful as shown in Fig. 9 where the particle velocities generated by parameter sets #1 to #8 are still very low or not having high enough particle temperature. Since Triplex II and Triplex Pro with 9 mm nozzle do not vary so much in performance, the 9 mm nozzle was then used with the Triplex Pro gun where variation of gun current can be easily done (Ref 18). Decreasing the Ar flow, decreasing the spray distance and increasing the current result in higher particle temperatures until parameter set #11 where the operational limitation of the TriplexPro gun has been reached. Temperatures above that of parameter set #16 (indicated by a broken line) were expected to produce molten particles since parameter set #16 was already proven to effectively deposit BMT coatings.

The process map for LAMT in Fig. 10 obtained by spraying with the Triplex II gun suggests that at 40/4 slpm Ar/He gas flow rate, 550 A of gun current and increasing spray distance until an optimum value of 200 mm, the particle temperature increases as particle velocity decreases due to longer residence time in the plasma plume. With this parameter set, BMT in Fig. 9 parameter set #15 has higher particle temperature due to lower heat capacity as compared to that of LAMT (Ref 5).

Figure 11 shows the particle temperature distributions of the powders measured using the standard spray parameters of 150 mm spray distance, gas flow of 45/6 slpm Ar/He but at varying gun power. In the normal Gaussian curves, the constant temperature of a bimodal particle distribution indicated by the solid vertical line in Fig. 11 is believed to be the melting temperature of the powder feedstock (Ref 19). For BMT (Fig. 11a), the constant mean temperature measured at ~2180 °C has a large discrepancy from the 3100 °C melting temperature

Table 1 Spray parameters for particle diagnostics

#	Gun	Ar, slpm	He, slpm	Current, A	Spray distance, mm
1	TriplexPro 6.5 mm	45	6	500	150
2	TriplexPro 6.5 mm	45	6	540	150
3	TriplexPro 6.5 mm	45	6	545	100
4	TriplexPro 6.5 mm	35	6	550	100
5	TriplexPro 6.5 mm	25	6	550	100
6	TriplexPro 6.5 mm	25	6	550	75
7	TriplexPro 6.5 mm	20	6	550	75
8	TriplexPro 6.5 mm	15	6	550	75
9	TriplexPro 9 mm	35	6	550	100
10	TriplexPro 9 mm	50	6	542	100
11	TriplexPro 9 mm	50	6	544	90
12	Triplex II	50	4	520	100
13	Triplex II	40	4	550	150
14	Triplex II	40	4	550	175
15	Triplex II	40	4	550	200
16	Triplex II	45	6	500	150

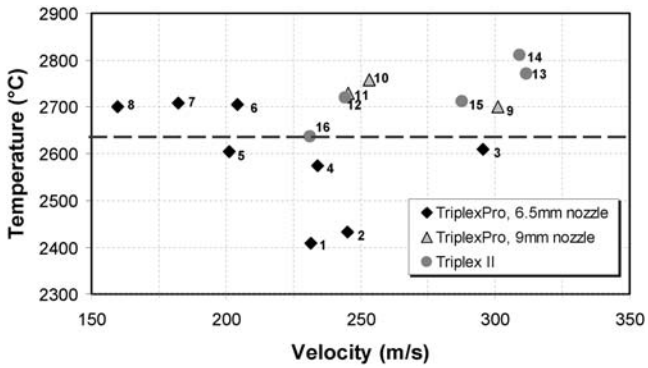

Fig. 9 Particle temperature-velocity process map for BMT generated using different plasma guns

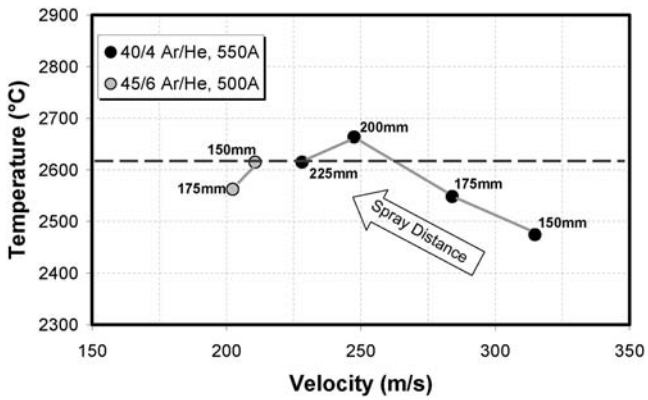

Fig. 10 Particle temperature-velocity process map for LAMT generated using Triplex II gun

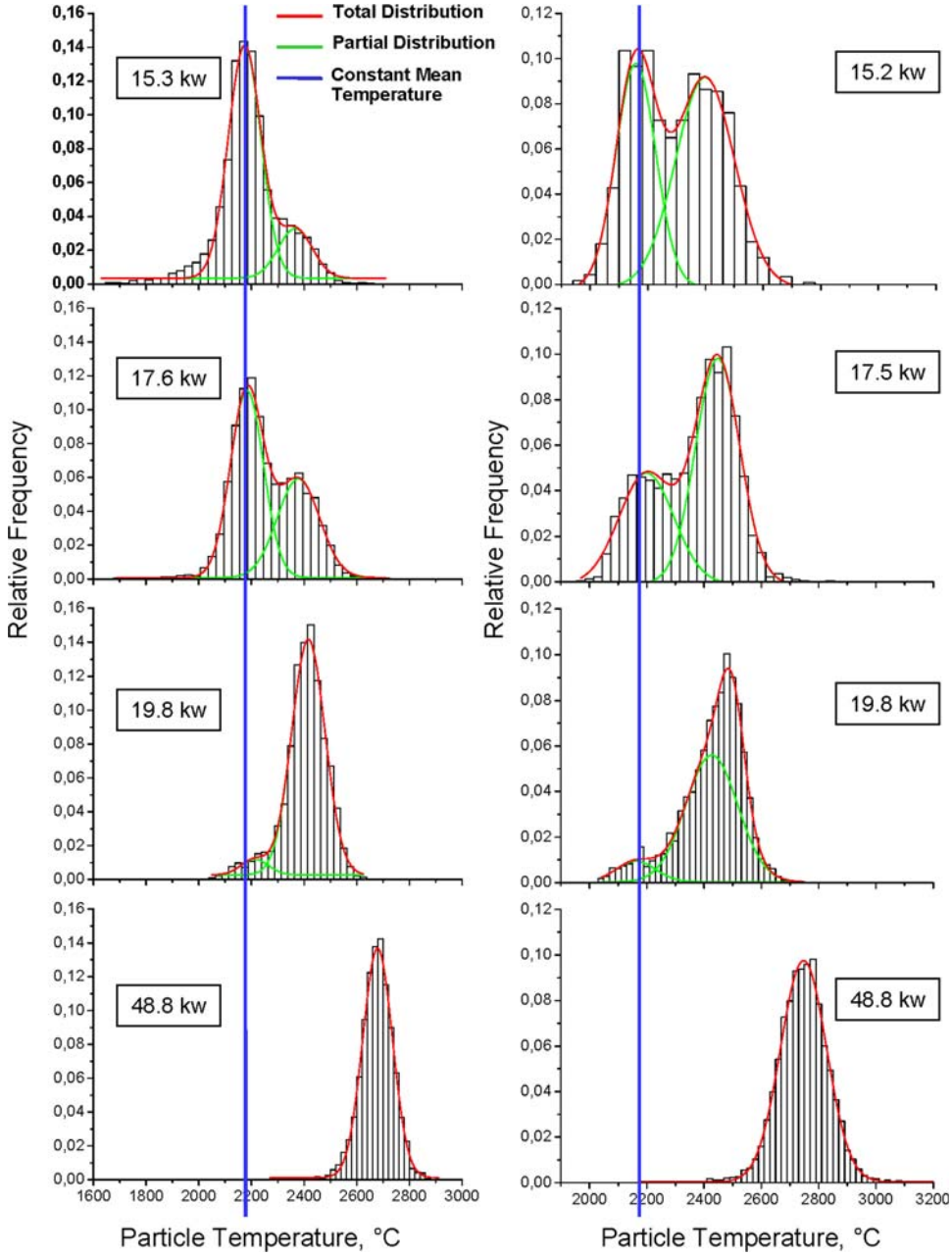

Fig. 11 Particle temperature distributions of (a) BMT and (b) LAMT measured using spray parameters of 150 mm stand-off distance, 45/6 slpm Ar/He gas flow and varying gun power

of BMT published in Ref 3 due to the limited absolute accuracy of the two-color pyrometry. This method of analysis is based on a gray body assumption and does not take into account the material dependent emissivity variation at the particular measurement wavelengths. Generally, emissivity values are unknown for most materials which hinder calculation of absolute melting temperature. The particles belonging to the constant temperature distribution are classified as solidifying and releasing their fusion enthalpy, while the particles in the distribution to the right of the indicator line are still molten. Similar concept applies to LAMT in Fig. 11b.

From the Gaussian distributions in Fig. 11, it is observed that for both BMT and LAMT the standard spray current used to deposit the coatings at 500 A corresponding to 48.8 kW gun power produced too hot particles which were still completely molten as they impact the substrate metal. This means that the particles stayed long enough at or above the melting temperature giving enough time for decomposition of phases to occur during particle flight. Gun current of 200 A (~15 kW) or possibly lower where majority of the particles have already solidified could probably prevent or minimize such decomposition and will be used for further investigations on

atmospheric plasma spraying of high melting temperature complex perovskites. Ongoing activities also include plasma spraying at stand-off distance shorter than 150 mm. Plasma spraying process will also be optimized to produce faster particle velocities as suggested from the process maps to reduce the particle residence time in the plume, but with sufficient particle temperature to attain good deposition efficiency.

4. Summary and Conclusions

Complex perovskite powders were deposited by atmospheric plasma spraying in thermal barrier coating systems. Plasma spraying $Ba(Mg_{1/3}Ta_{2/3})O_3$ and $La(Al_{1/4}Mg_{1/2}T_{1/4})O_3$ are accompanied by the formation of secondary phases which could not be avoided even with the addition of excess Ba and Mg in the starting composition to compensate for the amount lost during spraying. In-flight particle diagnostic results show that the standard parameters of 45/6 slpm Ar/He gas flow, 150 mm spray distance and 48.8 kW (500 A) gun power previously used to deposit coatings produced completely molten particles upon impact to the substrate metal which could have allowed the decomposition of phases. Gun power ~15 kW or lower is suggested to prevent the decomposition of phases since majority of the particles have already solidified upon impact to the substrate. In addition, it was also found that BMT complex perovskite coatings from sintered and crushed powders have longer thermal cycling lifetime than the coatings from agglomerated spray dried powders.

Acknowledgments

The authors are grateful to Mr. K.-H. Rauwald, Ms. M. Andreas, Dr. D. Sebold, Dr. W. Fischer, Mrs. S. Schwartz-Lückge and Mr. M. Kappertz of IEF-1 Forschungszentrum Jülich GmbH for their assistance in coating preparation and characterization and to Mr. J. Colmenares of Stony Brook University for valuable discussions on data analysis.

References

1. N.P. Padture, M. Gell, and E.H. Jordan, Thermal Barrier Coatings for Gas-Turbine Engine Applications, *Science*, 2002, **296**, p 280-284
2. A.S. Bhalla, R. Guo, and R. Roy, The Perovskite Structure—A Review of its Role in Ceramic Science and Technology, *Mater. Res. Innovat.*, 2000, **4**, p 3-26
3. R. Guo, A.S. Bhalla, and L.E. Cross, $Ba(Mg_{1/3}Ta_{2/3})O_3$ Single Crystal Fiber Grown by the Laser Heated Pedestal Growth Technique, *J. Appl. Phys.*, 1994, **75**, p 4704-4708
4. Y.-L. Kim and P.M. Woodward, Crystal Structures and Dielectric Properties of Ordered Double Perovskites Containing Mg^{2+} and Ta^{5+}, *J. Solid State Chem.*, 2007, **180**, p 2798-2807
5. M.O. Jarligo, D.E. Mack, R. Vassen, and D. Stöver, Application of Plasma Sprayed Complex Perovskites as Thermal Barrier Coatings, *J. Therm. Spray Technol.*, 2009, **18**, p 187-193
6. A. Ansar, G. Schiller, O. Patz, J.B. Gregoire, and Z. Ilhan, Plasma Sprayed Oxygen Electrode for Solid Oxide Fuel Cells and High Temperature Electrolyzers, *Thermal Spray 2008: Crossing Borders*, on CD-ROM, E. Lugscheider, Ed., June 2-4, 2008 (Maastricht, The Netherlands), DVS
7. G. Schiller, M. Müller, and F. Gitzhofer, Preparation of Perovskite Powders and Coatings by Radio Frequency Suspension Plasma Spraying, *J. Therm. Spray Technol.*, 1999, **8**, p 389-392
8. C. Zhang, W.-Y. Li, H. Liao, C.-J. Li, C.-X. Li, and C. Coddet, Microstructure and Electrical Conductivity of Atmospheric Plasma-Sprayed LSM/YSZ Composite Cathode Materials, *J. Therm. Spray Technol.*, 2007, **16**, p 1005-1010
9. G. Mauer, R. Vaßen, and D. Stöver, Comparison and Applications of DPV-2000 and Accuraspray-g3 Diagnostic Systems, *J. Therm. Spray Technol.*, 2007, **16**, p 414-424
10. W. Zhang and S. Sampath, A Universal Method for Representation of In-Flight Particle Characteristics in Thermal Spray Processes, *J. Therm. Spray Technol.*, in press
11. R. McPherson, The Enthalpy of Formation of Aluminium Titanate, *J. Mater. Sci.*, 1973, **8**, p 851-858
12. M. Vardelle, P. Fauchais, A. Vardelle, K. Li, B. Dussoubs, and N. Themelis, Controlling Particle Injection in Plasma Spraying, *J. Therm. Spray Technol.*, 2001, **10**(2), p 267-284
13. P. Fauchais, Understanding Plasma Spraying, *J. Phys. D: Appl. Phys.*, 2004, **37**, p R86-R108
14. R. Henne, Solid Oxide Fuel Cells: A Challenge for Plasma Deposition Processes, *J. Therm. Spray Technol.*, 2007, **16**, p 381-403
15. Y. Fang, A. Hu, Y. Gu, and Y.-J. Oh, Synthesis of $Ba(Mg_{1/3}Ta_{2/3})O_3$ Microwave Dielectrics by Solid State Processing, *J. Eur. Ceram. Soc*, 2003, **23**, p 2497-2502
16. C. Zhang, H.L. Liao, W.Y. Li, G. Zhang, C. Coddet, C.J. Li, C.X. Li, and X.J. Ning, Characterization of SOFC Electrolyte Deposition by Atmospheric Plasma Spraying and Low Pressure Plasma Spraying, *J. Therm. Spray Technol.*, 2006, **15**(4), p 598-603
17. R. Henne, T. Franco, and R. Ruckdäschel, High-Velocity DC-VPS for Diffusion and Protecting Barrier Layers in Solid Oxide Fuel Cells (SOFCs), *J. Therm. Spray Technol.*, 2006, **15**, p 695-700
18. G. Mauer, R. Vaßen, and D. Stöver, Preliminary Study on the Triplex Pro™-200 Gun for Atmospheric Plasma Spraying of Ytrria-Stabilized Zirconia, *Surf. Coat. Technol.*, 2008, **202**, p 4374-4381
19. G. Mauer, R. Vaßen, and D. Stöver, Detection of Melting Temperatures and Sources of Errors Using Two-Color Pyrometry During In-Flight Measurements of Atmospheric Plasma-Sprayed Particles, *Int. J. Thermophys.*, 2008, **29**, p 764-786